General Disclaimer

One or more of the Following Statements may affect this Document

- This document has been reproduced from the best copy furnished by the organizational source. It is being released in the interest of making available as much information as possible.

- This document may contain data, which exceeds the sheet parameters. It was furnished in this condition by the organizational source and is the best copy available.

- This document may contain tone-on-tone or color graphs, charts and/or pictures, which have been reproduced in black and white.

- This document is paginated as submitted by the original source.

- Portions of this document are not fully legible due to the historical nature of some of the material. However, it is the best reproduction available from the original submission.

"Raman Structural Studies of the Nickel Electrode"

(Power Systems Division)
(grant NAG 3-519)

SUMMARY REPORT

February 20, 1984 - March 20, 1985

B. C. Cornilsen

Michigan Technological University
Department of Chemistry and Chemical Engineering
Houghton, MI 49931

Sponsor:
University Grants Office
National Aeronautics and Space Administration
Lewis Research Center
21000 Brookpark Ave.
Cleveland, Ohio 44135

"Raman Structural Studies of the Nickel Electrode"

(Power Systems Division)
(grant NAG 3-519)

SUMMARY REPORT

February 20, 1984 - March 20, 1984

B. C. Cornilsen

Michigan Technological University
Department of Chemistry and Chemical Engineering
Houghton, MI 49931

Sponsor:
University Grants Office
National Aeronautics and Space Administration
Lewis Research Center
21000 Brookpark Ave.
Cleveland, Ohio 44135

CONTENTS

SUMMARY

It has been demonstrated that Raman spectroscopy is sensitive to empirically controlled nickel electrode structural variations, and that it has unique potential for structural characterization of these materials. Our goal is to understand how the structure relates to electrochemical properties, so that the latter can be more completely understood, controlled, and optimized. Electrodes have been impregnated and cycled at Michigan Tech, and cyclic voltammetry is being used for electrochemical characterization.

Structural variation has been observed which has escaped detection using other methods. Structural changes are induced by: i) cobalt doping, ii) the state of charge or discharge, iii) the preparation conditions and type of buffer used, and iv) the formation process.

We have demonstrated that charged active mass has an NiOOH-type structure, agreeing with X-ray diffraction results. Discharged active mass, however, is not isostructural with β - $Ni(OH)_2$. Chemically prepared α -phases are not isostructural either. A disordered structural model, containing point defects, is proposed for the cycled materials. This model explains K^+ incorporation. Band assignments have been made and spectra interpretted for β -$Ni(OH)_2$, electrochemical NiOOH and chemically precipitated NiOOH. The latter two compounds are isostructural.

I. INTRODUCTION and OBJECTIVES

The characterization of nickel electrode structures is essential to the development of improved electrodes, as well as for monitoring electrode properties during deposition, forming and cycling, i.e., quality control. The fundamental relationship between chemical structure and electrochemical properties demands improved structural understanding. Materials displaying different structures are formed because of variation in preparation conditions, cycling, varying applied potentials and dopant incorporation. We have demonstrated that laser Raman spectroscopy is a sensitive technique for characterizing these nickel electrode structures.

Our objective is to apply this structural tool to characterize the various structures and to develop a better understanding of the relation between the electrochemical properties and these structures. The various phases will be defined, their interrelations studied, and the mechanism of cobalt incorporation addressed, all in relation to the electrochemical properties. The role of potassium uptake and the structural changes occurring during the forming process itself are to be investigated as well.

II. Background

It is generally agreed in the literature[1-3] that two electrochemical cycles are observed for nickel electrodes, the α / γ cycle:

$$\alpha\text{-Ni(OH)}_2 \text{ ---> } \gamma\text{-NiOOH}$$

and the β / β cycle:

$$\beta\text{-Ni(OH)}_2 \text{ ---> } \beta\text{-NiOOH}$$

Ni(II) is oxidized to Ni(III) in each case, and the simple nomenclature, 2α , 3γ , 2β , 3β , distinguishes each electrochemical phase uniquely. A freshly deposited nickel hydroxide (chemically precipitated or electrochemically precipitated) is extensively hydrated, but the degree of hydration is variable and it is referred to simply as α-Ni(OH)$_2$.[2,3] The γ-phase, formed by charging the α-phase, is believed to be hydrated and to contain potassium (from the electrolyte). A 2α-phase is again formed upon discharge of the γ-phase. However, these phases and this α/γ cycle are not retained in cycled electrodes. Strong base transforms the α-phase to β-Ni(OH)$_2$, and charging then forms β-NiOOH.[3] It is possible to return to the α/γ cycle by overcharging a β/β cycle, to form γ-NiOOH.[1]

The process of cathodic, electrochemical precipitation of an α-Ni(OH)$_2$ from Ni(NO$_3$)$_2$ solution is called "deposition".[4] An electrode must be cycled a number of times (typically greater than 20) to make it "active" such that it demonstrates good electrochemical properties. This process is called "forming".

It is apparent, therefore, that the battery materials are not simply NiO. In high temperature NiO ($T > 900^{o}C$) a rhombohedrally distorted fcc structure is attained.[5] Each cation and anion is on a distorted octahedral site. No layers are formed. This structure is ordered antiferromagnetically and has a Néel temperature (T_N) of 523 K when not doped.[6] Dopants lead to a drop in T_N.[7] The ratio Ni/O is between 1.0000 and 0.9994 below ca. $1550^{o}C$; that is, the degree of nonstoichiometry is small compared to other binary transition metal oxides.[8]

Several key structural questions will be addressed in this study. We ask basically, what structural changes occur during the formation process and during cycling. For example, how do 2 β and 3 β differ structurally? Are the chemically precipitated model compounds really valid "models" for electrochemically active materials? The actual structures of the oxyhydroxide phases are not well defined, and whether the two γ -phases (formed from β-NiOOH at high potential) are the same as γ formed from α is not firmly established. There is also disagreement as to whether these cycles, α/γ and β/β , traverse a series of solid solutions or a mixture of two phases upon charging and discharging.[9,10]

Additives such as cobalt or lithium improve electrochemical performance. Cobalt doping improves electrode performance by extending battery life (i.e. providing a greater number of cycles), increasing charge acceptance, and increasing the overpotential of the oxygen evolution reaction.[11] Greater depth of discharge is obtained because of increased ionic and

electronic conductivity.[12] Why dopants influence the properties in this way and the detail of how cation dopants might be structurally incorporated are unknown. It is possible that dopants stabilize (or destabilize) certain structures. Lithium, often added to the electrolyte, is an example of an additive which can increase capacity, yet it can also be detrimental to performance.[1]

The Structures of Layered Nickel Hydroxides

Electrochemically cycled "active mass," chemically precipitated hydroxides, and electrochemically deposited (i.e., cathodically deposited) materials (Table I) are believed to have layered structures.[1] NiO_2 layers are formed from a pair of close-packed planes of oxygen atoms, containing interstitial nickel atoms. These NiO_2 layers are analogous to layered CdI_2 or $CdCl_2$, except that protons, metal cations, and water molecules can be intercalated between layers (interlamellar). Comparisons of X-ray powder diffraction patterns for electrochemical active mass and those for precipitated materials indicate structural similarities, and these two types of materials are in general believed to be related.[1-3,13]

Of all the compounds and materials discussed in relation to nickel active mass, only the β -$Ni(OH)_2$ structure is well defined by single crystal X-ray and neutron diffraction studies.[14,15] This phase has a layered CdI_2 type structure (also called the brucite, $Mg(OH)_2$, structure) with ABAB... stacking of the oxygen planes. The protons are each covalently bonded to only one oxygen atom. A correct view of this structure must recognize

that not only oxygen and hydrogen are covalently bonded, but also the nickel and oxygen atoms. NiO_2 planes are staggered so that the oxygens facing the interlamellar protons do not align. This allows no hydrogen bonding; and, in particular, no O-H-O bonds are found in this ordered β-$Ni(OH)_2$ crystal structure (with 4.60 Å interplanar spacing).[14,15]

Interlamellar water molecules can distort this ideal, ordered structure, and both long-range and short-range interlayer stacking order can be lost. The so-called α-$Ni(OH)_2$ structure is believed to be disordered in this fashion.[1,3] In general the term α-phase is used to refer to any hydrated $Ni(OH)_2$. Bode et al. have characterized a unique α-phase with X equal to 0.66 (in $Ni(OH)_2 \cdot XH_2O$).[3] In practice, X can vary with preparation conditions, and this plus typically poor crystallinity leaves this compound ill-defined. The literature often refers to hydrated materials as "α-$Ni(OH)_2$", without greater clarification. Therefore, reference to an "α-phase" may not necessarily imply that the Bode et al. structure is present. Further research is required to define the variability exhibited by these so-called α-phases.

It is emphasized that water molecule intercalation is only one of the forms of disorder inherent in a layered lattice. Another degree of disorder is introduced by different types of layer stacking. For example NiO_2 layers can stack in an ABCABC... series in the so-called $CdCl_2$ type lattice or an ABBCCA... series.

The generally accepted model structure for charged active mass is the oxyhydroxide structure, MOOH (or HMO_2). This structure is known for other transition metal oxyhydroxides as well. It has been proposed for charged active mass on the basis of powder diffraction pattern similiarities with oxidatively precipitated β - and γ-NiOOH.[1,3,13,16] This structure differs from that of β-$Ni(OH)_2$ in that the layer stacking places adjacent oxygens over one another allowing formation of linear O-H-O bonds (with 4.85 Å interplanar O-O spacing).[13,16] There are, of course, only half as many interlamellar protons as well.

The literature refers to 2β-, 2α-, 3β-, and 3γ-active mass, and analogy is made to the above α-, β-, and γ-structures of $Ni(OH)_2$ and NiOOH. Structural differences between the electrochemical materials and the chemically precipitated materials have not been distinguishable on the basis of X-ray powder diffraction data because of the structural similarities of all of these layered compounds and typically poor crystallinity. Subtle differences in powder patterns may reflect significant structural differences.

Structural Interpretation

The first half of any spectral study involves careful variation of variables (in this case electrochemical) to correlate any spectral changes. The second half involves "band assignment" and "spectral interpretation" based on careful experiments which identify the structure-spectrum correlation. These can often include spectral analysis of samples with known structures, of isotopically substituted samples (e.g., D/H or $^{*}Ni/Ni$), doped

samples, etc. Spectra of isostructural materials can also be a great aid in making band assignments.

A Raman spectral study requires a solid data base upon which significant spectral variations can be defined. With the latter information, the origins of the spectral changes can be defined allowing complete understanding of the empirical variations first observed. Careful experiments must be made to allow "band assignments" so that structural information can be extracted from the data. For example, an experiment demonstrating a spectral change originating from a particular change in variable, such as cobalt content, characterizes or fingerprints the change. Measurement of the cobalt content is important in itself; but even more importantly, detailed information about the structural origin of this change will allow understanding of the mechanism of cobalt incorporation and its influence on electrode properties.

Prior to this work only one Raman paper, by J. F. Jackovitz, reported spectra of electrode materials.[17] IR spectra were reported previously by Kober.[18,19] Spectral analysis in terms of the structure has only been done for the ordered β-$Ni(OH)_2$.

Experimental

The experimental data presented demonstrate that high quality Raman spectra can be reproducibly obtained for electrode materials. Both the green and the black nickel electrode materials require multiple scan (signal averaged) data collection to obtain high signal-to-noise ratio Raman spectra. Most colored materials are sensitive to laser heating and can decompose on

long exposure to the laser beam; therefore, low laser intensities must be used to obtain quality data, and longer scan times become necessary to obtain good signal-to-noise ratios. A typical 6-scan spectrum from 50 cm^{-1} to 4000 cm^{-1}, for one sample, requires 8 hours. Longer times, 20 scans and 26 hours, are required for the black samples which absorb more incident laser intensity and are less intense Raman scatterers. They may also be more sensitive to laser heating and dehydration (dehydroxylation) so that lower laser intensities are required. It should be added that the structural characterization of fine particle size, polycrystalline materials, which may exhibit some noncrystallinity, is, in general, difficult. Raman spectroscopy is ideal for the study of these types of materials.

III. RESULTS AND DISCUSSION

Deposited Materials

In the initial stages of this research a variety of deposition techniques were used to prepare hydrated nickel hydroxides. Unlike active mass, these materials are generally green. As depicted by the Raman spectra in Figures 1 and 2, the structures vary considerably, depending on preparation variables. Spectra chosen for use in these figures demonstrate that chemically precipitated material (Figures 1a and 2b) and cathodically deposited material (Figures 1b, 1c and 2a) differ in structure. Furthermore, the addition of cobalt (Figure 1d) introduces a distinct spectrum indicating significant structural variation. Note that the 460 cm^{-1} band is weaker than the bands near 530 cm^{-1} in this case. Figures 1b and 1c demonstrate how EtOH (ethanol) and NO_2^- buffers influence the spectra. They, too, introduce structural change. In general the vibrational modes below 700 cm^{-1} are lattice modes involving primarily nickel atom and oxygen atom motions. Vibrational bands in the 700-1500 cm^{-1} region are nitrate (NO_3^-) or nitrite (NO_2^-) group vibrations. These anions are occluded during deposition and are readily observable using this technique. It would be possible to quantitatively determine these anion concentrations if standards were prepared. In the 3300-3800 cm^{-1} region, O-H stretching modes are observed (Figure 2) for waters of hydration and hydroxide anions. This region of the spectrum exhibits a significant change if a deposited material stands in base (compare Figures 2b and 2c). The broad 3650 cm^{-1} band decreases.

The literature reports that H_2O is removed from the hydrated $Ni(OH)_2$ lattice upon standing in base.[3] This observation allows assignment of this broad 3650 cm^{-1} band to the O-H stretch of interlamellar water molecules in the lattice. Broad vibrational bands have also been observed in this region for physi- or chemisorbed water in layered, silicate minerals.[20] This probably includes interlamellar water molecules. Certainly in our case, the latter can be proposed since interlamellar water molecules are believed to be present in both chemically precipitated and cathodically deposited, hydrated α -nickel hydroxides.[3] Broadened water modes are often interpreted as reflecting extensive hydrogen bonding. Hydroxide groups in layered minerals are known to produce sharp vibrational modes in the 3600 cm^{-1} region, suggesting these remaining sharp modes are of hydroxyl stretching origin.[20]

In general it can be seen that both the lattice mode and O-H stretch regions of the Raman spectra reflect significant structural variations for chemically precipitated and cathodically deposited (α -type) materials.

Electrochemical Phases

Spectra of charged electrodes, Figure 3a and 3c, exhibit only two vibrational bands in the Raman spectrum. No O-H stretching modes appear above 3000 cm^{-1}. Interestingly, no new spectral features appear upon discharging (Figure 3b and 3d). Only frequency shifts and intensity changes are observed.

These materials were each prepared under electrochemical conditions (i.e., cycled) to give the defined phases according to literature methods and conditions.[3,4,16,21,22] Figure 3a is a spectrum of a charged plaque electrode (3β) prepared here at MTU (cobalt-free) using NASA conditions (20% KOH, nitrite buffer). It was charged to 0.470 V after cycling provided a β/β cycle.[21] The same electrode, discharged to -0.2 V to give 2β, is depicted in Figure 3b. Overcharging a plaque electrode (20% KOH, 45% ethanol buffer) gave a spectrum of a γ-phase (Figure 3c). Thin film γ-phase active mass on nickel foil gives a similar spectrum. An initial spectrum on a thin film on nickel foil that was cycled at low pH (MacArthur's method[22]) provides an α-phase spectrum (Figure 3d).

Cycling these electrodes definitely influences the spectra; β/β and α/γ cycles are distinct. We are currently quantifying the spectral variation in relation to cycling and specific charging conditions. It is interesting to note that the electrochemical 2β spectrum is not the same as that for α-$Ni(OH)_2$ nor β-$Ni(OH)_2$. The latter spectra will be discussed in the next section of this report. Most significant is the fact that the spectra of charged and discharged active mass are similar (Figure 3), i.e., they obey similar spectral selection rules. This indicates they have very similar structures.

Significant structural changes occur in the lattice mode region when a deposited material is put in basic solution and charged. Figure 4 shows how the spectrum of a cathodic, cobalt-containing precipitate (Figure 4a) changes upon standing in KOH

(Figure 4b) and then upon charging (Figure 4c). These significant intensity changes reflect structural differences.

Comparison with cobalt-free spectra demonstrates that the cobalt in the latter materials influences the structure of both the deposited phase and the cycled material. The detailed structural changes accompanying cobalt incorporation have not been worked out in detail yet, and further work on cobalt containing electrodes is planned. How the structure of the deposited materials influences that for the charged material is of import since we wish to optimize the latter.

Two spectra from an Eagle Picher (as-received and partially charged) plaque electrode are depicted in Figure 5. That of the black material (Figure 5a) is typical for a partially charged material and similar to those in Figure 3. That of a green area on the surface is different (Figure 5b). This spectrum shows that this green area was not charged, i.e., not in electrical contact with underlying active mass. It is identical to that observed previously for an as-deposited (not formed nor cycled), cobalt containing α-phase (Figure 1d). This suggests an application of Raman spectroscopy to quality control of electrodes. More importantly, this result substantiates that the two bands at low frequency are observed in a commercial electrode as well. This is in contrast with a recent report of only one broad Raman band obtained for a commercial electrode material.[23]

In short, both the formation process and cycling change the structure of nickel electrode materials. Cobalt doping also influences the structure. To understand the structural

significance of the spectral changes observed we must next consider the IR and Raman spectra of defined phases and consider theoretical selection rules predicted by factor group analysis for known or hypothetical structures.

β-$Ni(OH)_2$

The Raman spectrum of ordered β-$Ni(OH)_2$ is given in Figure 6c. There is one Raman active O-H stretch (3580 cm^{-1}), and there are two strong lattice modes (448 and 312 cm^{-1}). A third lattice mode (378 cm^{-1}) is visible at low temperature (13 K). These four bands agree with the predicted selection rules for the D_{3d}^3-$P\bar{3}m$ space group (see Table 2). These selection rules were first predicted by Mitra[24-25], used by Kober[18-19], and later reiterated by Jackovitz.[17] Our infrared spectrum of β-$Ni(OH)_2$ is in agreement with several IR studies of this material including Figlarz and Le Bihan, Houalla et al., Kober, and Jackovitz.[17-19,26,27]

We have observed that both the broad IR band and broad Raman band (at ca. 3440 and 3650 cm^{-1}, respectively) increase or decrease depending on the adsorbed, interlamellar water content (monitored via TGA). This water (< 8 % by weight) is lost at ca. 100° C (maximum of differential TGA peak) whereas $Ni(OH)_2$ degrades thermally to NiO and H_2O at 350° C. Therefore these bands represent interlamellar water. Figlarz and Le Bihan observed a decrease in this IR band as interlamellar water was removed from turbostratic $Ni(OH)_2$.[26]

The water content depends upon the preparation method. The anhydrous, ordered β-$Ni(OH)_2$ material was prepared by Barnard's

method, recrystallization from an NH_4^+ complexed nickel solution over H_2SO_4.[28] The first precipitate of β-$Ni(OH)_2$, which contains more of this excess water, produces a unique TGA pattern with a characteristic lower temperature H_2O loss (2 to 8 %) at ca. 90° C and hydroxide loss anywhere between 285° and 350° C.

When low levels of H_2O are occluded during the precipitation, the Raman spectrum displays additional bands in the OH stretch region at 3687 cm^{-1}, 3650 cm^{-1}, and 3600 cm^{-1}, and in the lattice mode region at 515 cm^{-1} (Figure 6a). The IR spectrum does not visibly change in the lattice mode region. Only the above mentioned broad band at 3440 cm^{-1} changes.

These bands are not present in ordered β-$Ni(OH)_2$ (Figure 6c). Furthermore, the bands at 3687 cm^{-1} and 515 cm^{-1} decrease in intensity upon evacuation in a cryostat at 13 K (Figure 6b). They do not reappear after warming to room temperature and are, therefore, not temperature dependent modes. They appear to be related to a species that is desorbed upon evacuation. Tentatively we associate them with interlamellar water loss under vacuum. The band at 3600 cm^{-1} does not change under vacuum and we therefore assign it to a mode activatd by ABC stacking of the NiO_2 layers which may activate an additional O-H stretching mode.

Jackovitz's assignment of the Raman bands at 519 cm^{-1} (similar to our 515 cm^{-1} band) and 3599 cm^{-1} (our 3600 cm^{-1} band) for β-$Ni(OH)_2$ is therefore inconsistent with our results.[17] He did not report Raman bands at 3580 and 3687 cm^{-1}.

Comparison of the spectra for electrochemical 2 β (discharged active mass) (Figure 3) and for both ordered and

disordered β-$Ni(OH)_2$ (Figure 6) demonstrates a very important fact. Discharged 2β is not structurally the same as β-$Ni(OH)_2$. Furthermore, the similarity of the spectra for charged and discharged active masses shows that they have a related structure. In the next sections we shall interpret spectra of the charged phase and propose a structural model which explains the similarities.

γ-NiOOH

The structures of a chemically oxidized precipitate (NiOOH)* and an electrochemical 3γ phase are compared in Figures 7 and 8, containing the Raman and IR spectra, respectively. The spectra are identical indicating these two phases are isostructural.

The 3γ was prepared by MacArthur's method,[22] i.e., overcharging a thin film on nickel foil or overcharging a plaque electrode. (The Raman spectra are similar for both electrode types.) The structure of the precipitated material has been determined to be NiOOH.[13,16,29-32] The 3γ and the latter material have been declared isostructural on the basis of powder X-ray diffraction data.[13,16,31,32] Our results confirm this structural similarity. We therefore disagree with Melendres and Xus' recent conclusion that active mass is not isostructural with NiOOH.[23] Furthermore, as mentioned above, the discharged materials display similar selection rules.

Most importantly, these spectra can be interpreted by the selection rules predicted for a unit cell with a single formula

* Prepared by Dr. Dean C. Luehrs in our department via sodium hypochlorite oxidation of $Ni(NO_3)_2$. Analysis of this material gives a structural formula $Ni_{0.81}K_{0.13}Na_{0.06}O_{1.17}\cdot 0.94H_2O$.

unit (Z = 1) of NiOOH with a D_{3d}^5 - $R\bar{3}m$ space group. This space group has been reported for MOOH compounds with M = Cr and Co.[33,34] Two Raman and two IR active lattice modes are predicted, and two IR active O-H stretching modes are predicted (see Table 2). No coincidences are predicted (nor observed). Most important is the fact that no Raman active OH stretching modes are predicted or observed. This supports our argument that Z is one for this unit cell of NiOOH. If the unit cell ($Z \geq 2$) were larger, the O-H stretches would become Raman active. We see no such activity, not even at lower frequencies as seen for the IR active O-H stretches at 1390 cm^{-1} and 1455 cm^{-1}. Varma et al. report two Raman bands for an anodized electrode, at 1333 and 1404 cm^{-1}.[35] They do not or could not report the lower energy doublet at 555 and 475 cm^{-1}. This was a spectrum of anodized α - phase. It was not formed or cycled. We see Raman bands in the 1300 to 1420 cm^{-1} region (not necessarily simultaneously) for uncycled electrodes and assign these to NO_3^-, NO_2^-, or $CO_3^=$ impurities. We have not seen these bands after cycling and, therefore, do not believe them to be O-H stretches of the NiOOH lattice.

These NiOOH compounds are therefore isostructural with CoOOH and CrOOH. The latter are known to contain very short O-H-O bonds, and IR spectral analyses have been carried out.[33,34] The fact that the X-ray data for these materials has been interpreted in terms of larger unit cells is simple to understand. Impurities (such as K^+) and point defects (Ni vacancies) can influence the time averaged or spatially averaged

atomic positions as measured in a diffraction experiment, making the unit cell "appear" larger. Averaging of two partially filled sites can introduce an "apparent" atom on a site halfway between the two. Vibrational spectra can unravel this apparent discrepancy.[36] With single crystal data and consideration of the proper defect model, the X-ray data can be explained successfully as well.[37]

Therefore, we conclude that the active mass spectra indicate a structure for charged and discharged mass that is based upon the NiOOH, D_{3d}^5-$R\bar{3}m$ space group.

Structural Model of NiOOH and NiOOH(H)

On the basis of the Raman and IR spectral selection rules observed for active mass (discharged as well as charged), the ABBCCA type structure of NiOOH appears to be maintained upon discharge. We have found no true β-$Ni(OH)_2$ with an ABAB structure in the cycled electrochemical systems. A defective model can potentially explain this observed fact as well as several other important experimental facts. The latter include: 1) incorporation of K^+ and the difference between α/γ and β/β cycles, 2) the similarity of 3β and 2β X-ray diffraction powder patterns, 3) the black color and high conductivity of both discharged and charged phases, 4) the maximum average oxidation state observed for nickel upon full charge, and 5) the observed empirical formulae for charged and discharged phases (i.e., the Ni/O or apparent Ni/H_2O ratios).

The ideal 2NiOOH structure can be and is often written as $Ni_2O_3 \cdot H_2O$. Most empirical formulae for γ- or β-NiOOH materials

given in the literature cannot be written this simply because of items 1 and 4 above. Since no H_2O type vibrational modes are observed in IR or Raman spectra, a hydrated structure is not believed to be an accurate representation. The empirically observed water content (in other words, the observed $O^=$ and OH^- content) can be properly incorporated into the NiOOH structure by simply including cation (nickel) vacancies, V_{Ni}. One cation site is formed per pair of oxygen sites in this structure (Ni_{Ni} + 2 O_O). The number of vacancy sites, x, is simply the difference between the number of nickel sites (1-x) and the number of pairs of oxygen sites (1). The formulae in Table 3 have been cast from literature data into this form. Then the stoichiometric amount of protons (from the empirical formulae) is incorporated. First one mole of protons are placed on interlamellar hydrogen sites, H_H, of the $Ni_{1-x}V_{Nix}OOH$ lattice (i.e., between two oxygen atoms of adjacent layers). Then remaining protons can be placed either in the interlamellar space or placed on nickel vacancy sites. Three protons can be placed on each Ni(III) site. Two on each Ni(II) site. This model explains how protons and potassium cations can be incorporated in simple fashion. Protons in the interlamellar space hydrogen-bond to hydroxyl groups to effectively form water molecules in the interlamellar space. These different types of hydrogen sites explain the complex thermogravimetric analysis patterns observed for these materials.

The maximum oxidation state observed for nickel in charged active mass is 3+ per site. For a lattice with 75% of the nickel sites occupied (i.e. 25% vacancies), each nickel atom is

effectively in a 4+ oxidation state upon ionization of the vacancy sites. This gives an average oxidation state of 3.0 per cation site. If K^+ is incorporated, an equal amount of Ni^{3+} is formed from Ni^{2+} sites (discharged) or an equal amount of Ni^{4+} is formed from Ni^{3+} sites (charged), thereby increasing the apparent, average oxidation state of Ni even further. This explains the maximum average empirical oxidation state observed for charged phases or chemically oxidized precipitates.

Furthermore, the black color of both charged and discharged active mass is understandable because of the large point defect content in the proposed structure. It is well known that defective materials absorb light across the visible region. Chemically precipitated materials are bright green in contrast. This defect structure also explains the sizeable electrical conductivities observed for electrode active mass. To test our model further, we shall compare empirical data in the literature with the predictions based on this defective model as we continue this study.

IV. CONCLUSIONS

Our purpose has been to characterize the various structures formed in nickel electrode materials, and to correlate these with the electrochemical properties. Electrochemically induced structural changes have been observed using Raman spectroscopy. Structural variation has been observed which has escaped detection using other methods. A variety of structural changes are induced by the preparation method (chemical or electrochemical), type of buffer used, the formation process, charge state, and cycling. Cobalt additives influence both the structure of the deposited material and that of formed, active mass.

Vibrational spectra for two model compounds, β-$Ni(OH)_2$ and NiOOH, have been completely interpreted. These compounds were prepared by literature methods. Spectra for ordered β-$Ni(OH)_2$ obey selection rules predicted for this well known, brucite crystal structure. Selection rules for charged active mass have been successfully predicted on the basis of a single unit cell, NiOOH structure. This is essentially in agreement with powder X-ray diffraction results although a smaller and disordered unit cell is supported by our data. We find that chemically prepared and electrochemically prepared NiOOH have essentially the same structure. K^+ incorporation does not change this structure type as reflected by the fact that the selection rules do not change. A structural model containing point defects is proposed that explains both the mechanism of K^+ retention and the empirical formulae reported for nickel oxyhydroxides.

Most importantly, a unique structure for discharged active mass is indicated by the spectra, which can be interpretted in terms of a reduced, defective NiOOH structure. This structure is more closely related to the charged phase than to the ordered β-$Ni(OH)_2$ structure. The defect model explains the formation of this discharged structure in a simple fashion; protons are incorporated on nickel vacancies and/or in the interlamellar space. This model also explains a variety of other empirical characteristics of these materials.

Furthermore, the so-called α -phases prepared via several different hydroxide precipitation techniques, including cathodic deposition, are not isostructural with electrochemical 2 β , nor with electrochemical 2 α phases. The current results indicate that further research should allow definition of how additives are incorporated.

V. FUTURE WORK

We shall continue to prepare and characterize the structures of unique phases defined in the literature. These have been defined by other structural studies and/or electrochemically, e.g. via cyclic voltammetry. The structural differences between electrochemically "activated" and deactivated" materials will be defined.

Cycled electrodes will be studied to characterize structural changes that occur with very high cycling. Electrodes cycled and characterized by other methods at NASA-Lewis will be studied.

Correlation of our structural results from the Raman and IR vibrational studies with that of X-ray diffraction, cyclic voltammetry, and thermogravimetric analyses will be continued. This is important to relate our structural results to previous structural and electrochemical data in the literature.

The unique structural changes occuring during charging, discharging, and cycling will be studied to define them in greater detail. The variations in spectral parameters will be quantified. This will help to define differences due to potassium, lithium, and cobalt incorporation and differences between alpha/gamma and beta/beta cycles. We will investigate how additives influence electrode electrochemical properties.

The defect model proposed will be tested by comparing it to the quantitative spectral results.

An in-situ study will be carried out to allow comparison

with other structural data already collected for free electrodes. Here the influence of controlled potential and information about electrode self-discharge can be defined.

V. REFERENCES

1. P. Oliva, J. Leonardi, J. F. Laurent, C. Delmas, J. J.Braconnier, M. Figlarz, F. Fievet and A. de Guibert, J. Power Sources, 8, 229-255 (1982).

2. R. G. Gunther and S. Gross, editors, Proc. Symposium on the Nickel Electrode, Electrochemical Society, Pennington, N.J., 1982.

3. H. Bode, K. Dehmelt, and J. Witte, Electrochimica Acta, 11, 1079-1087 (1966).

4. a) M. B. Pell and R. W. Blossom, U.S. Patent 3,507,699, April 21 (1970); b) D. F. Pickett, U.S. Patent 3,827,911, Aug. 6 (1974).

5. a) H. P. Rooksby, Acta Cryst., 1, 226 (1948); b) N. C. Tombs and H. P. Rooksby, Nature, 165, 442 (1950).

6. G. A. Slack, J. Appl. Phys., 31, 1571 (1960).

7. E. F. Funkenbusch and B. C. Cornilsen, Solid State Commun., 40, 707 (1981).

8. a) C. M. Osburn and R. W. Vest, J. Phys. Chem. Solids, 32, 1331 (1971); b) B. C. Cornilsen, E. F. Funkenbusch, C. P. Clarke, P. Singh, and V. Lorprayoon, Advances in Materials Characterization, edited by R. A. Condrate, D. Rossington and R. Snyder, Plenum Press, 1983, pp. 239-248.

9. B. E. Conway and E. Gileadi, Canad. J. Chem., 40, 1933 (1962).

10. R. Barnard, C. F. Randell, and F. L. Tye, J. Electroanal. Chem., 119, 17 (1981).

11. M. E. Folguer, J. R. Vilche, and A. J. Arvia, J. Electroanal. Chem., 172, 235 (1984).

12. A. H. Zimmerman and P. K. Effa, J. Electrochem. Soc., 131, 709 (1984).

13. H. Bode, K. Dehmelt and J. Witte, Z. anorg. Chemie, 366, 1-21 (1969).

14. W. Lotmar and W. Feitknecht, Z. Krist., 93A, 368 (1936).

15. A. Szytula, A. Murasik, and M. Balanda, Phys. Stat. Sol. B,, 43, 125 (1971).

16. O. Glemser and J. Einerhand, Z. Elektrochem., 54, 302 (1950).

17. J. F. Jackovitz, Proc. Symp. on the Nickel Electrode, edited by R. G. Günther and S. Gross, Electrochemical Society, Pennington, N.J., 1982, p. 48.

18. F. P. Kober, J. Electrochem. Soc., 112, 1064 (1965).

19. F. P. Kober, J. Electrochem. Soc., 114, 215 (1967).

20. R. G. J. Strens, "The Common Chain, Ribbon, and Ring Silicates," in The Infrared Spectra of Minerals (V. C. Farmer, ed.), Mineralogical Society, London, 1974, pp. 305-330.

21. R. Barnard, G. T. Crickmore, J. A. Lee, F. L. Tye, J. Applied Electrochem., 10, 61 (1980).

22. D. M. MacArthur, J. Electrochem. Soc., 117, 422 (1970).

23. C. A. Melendres and S. Xu, J. Electrochem. Soc., 131, 2239 (1984).

24. S. S. Mitra, Z. Kristall., 116, 149 (1961).

25. S. S. Mitra, Solid State Physics, 13, (F. Seitz and D. Turnbull, eds.), pp. 1-80, (1962).

26. M. Figlarz and S. Le Bihan, C. R. Acad. Sc., Ser. C, 272, 580 (1971).

27. M. Houalla, V. Perrichon, and P. Turlier, C. R. Acad. Sci., Ser. C, 284, 1 (1977).

28. R. Barnard, C. F. Randell, and F. L. Tye, Power Sources 8, (J. Thompson, ed.), Academic Press, London, 1981, p.401.

29. O. Glemser and J. Einerhand, Z. anorg. Chemie, 261, 26 (1950).

30. O. Glemser and J. Einerhand, Z. anorg. Chemie, 261, 43 (1950).

31. D. Tuomi, J. Electrochem. Soc., 112, 1 (1965).

32. R. S. McEwen, J. Phys. Chem., 75, 1782 (1971).

33. R. G. Delaplane, J. A. Ibers, J. R. Ferraro, and J. J. Rush, J. Chem. Phys., 50, 1920 (1969).

34. J. J. Rush and J. R. Ferraro, J. Chem. Phys., 44, 2496 (1966).

35. R. Varma, G. M. Cook, N. P. Yao, "Raman Spectroscopy for In-situ Monitoring of Electrode Processes," ANL/OEPM-82-2, Argonne National Laboratory, Argonne, IL, 1982.

36. B. C. Cornilsen and R. A. Condrate, J. Phys. Chem. Solids, 38, 1327-1332 (1977).

37. B. E. Robertson and C. Calvo, Can. J. Chem., 46, 605-612 (1968).

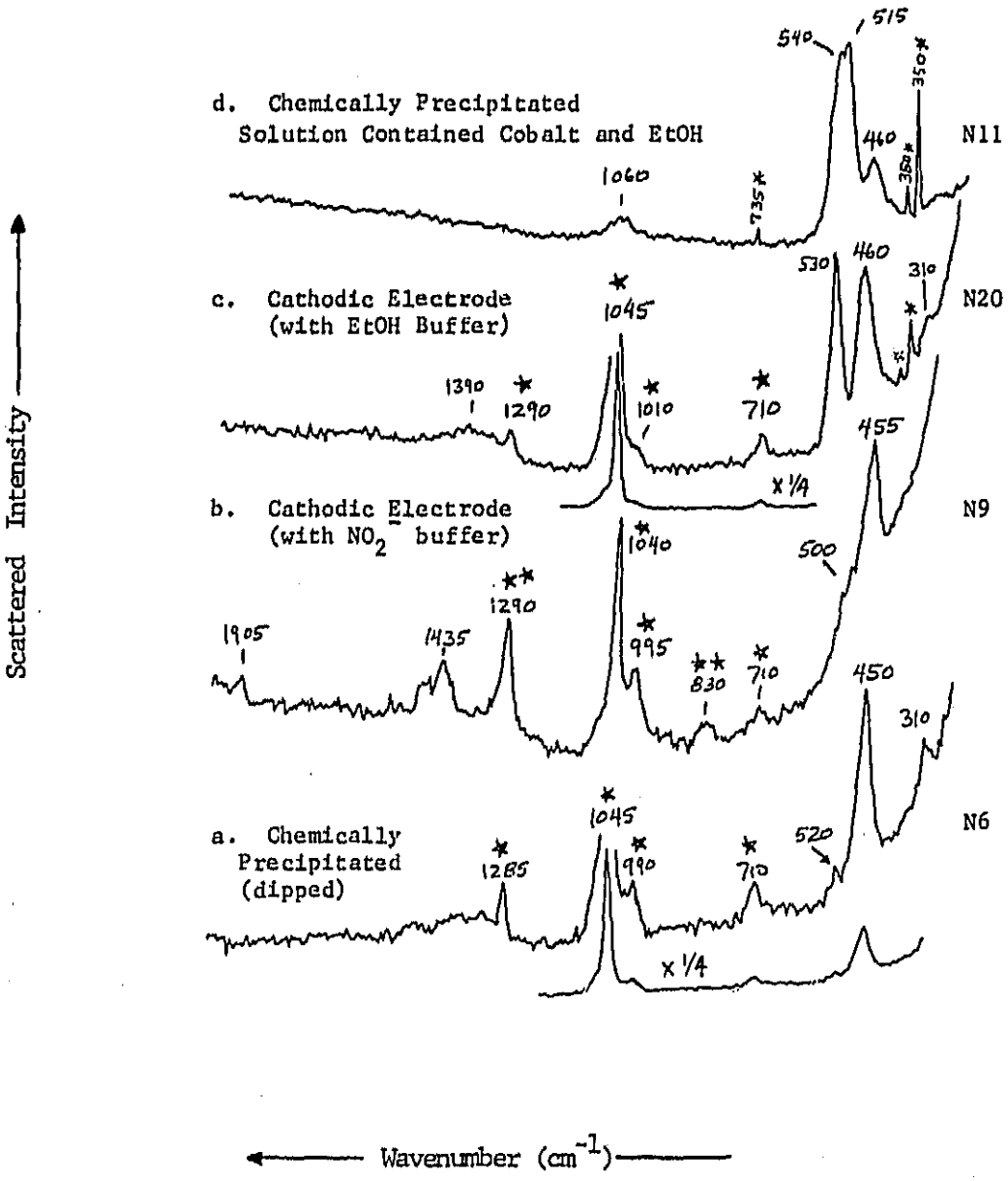

Fig. 1. 2000 - 300 cm^{-1} region of Nickel Hydroxide Materials.
* NO_3^- bands, ** NO_2^- bands, *Plasma Lines.

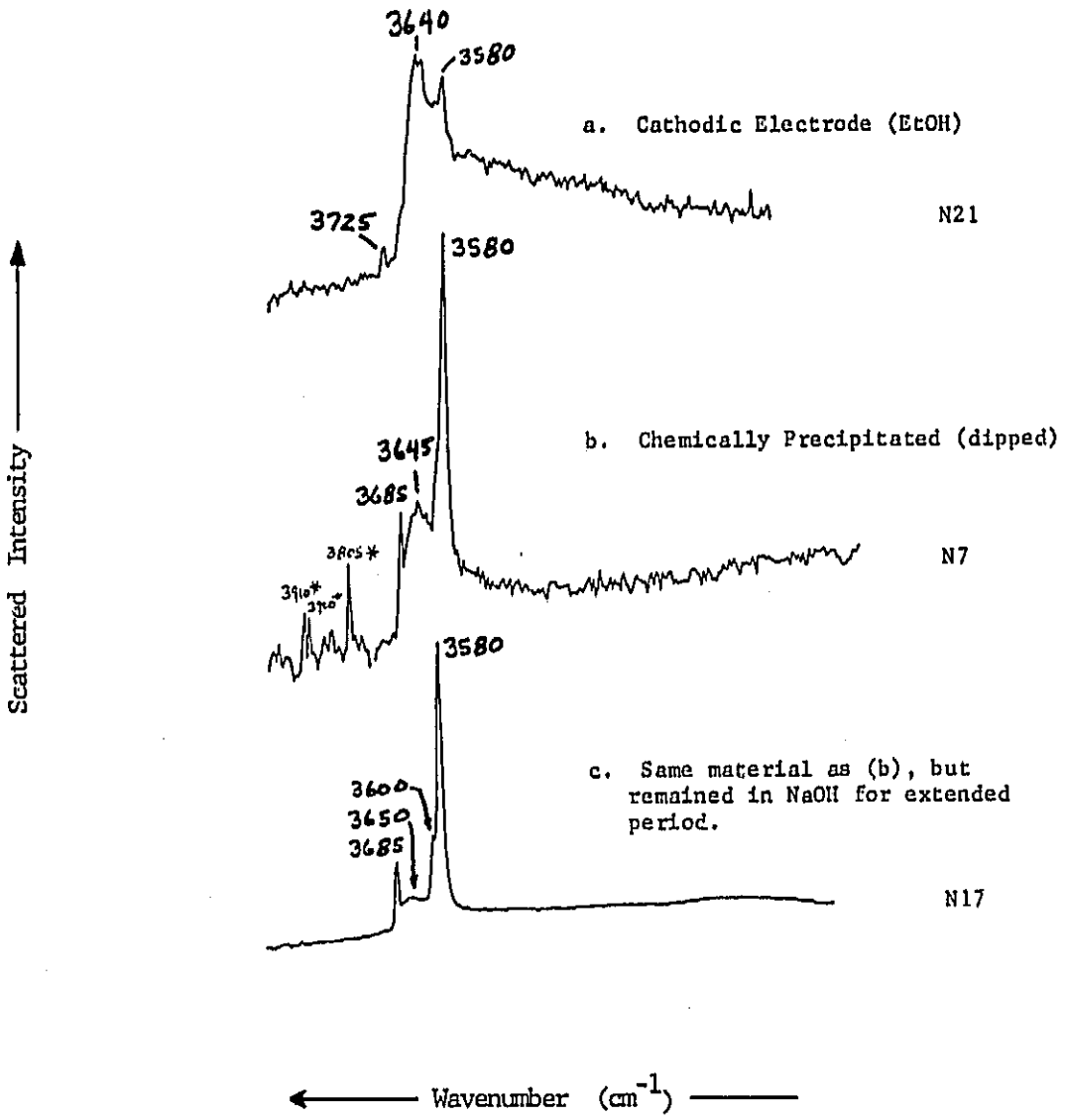

Fig. 2. OH-stretch region of Nickel Hydroxide materials.
*Plasma Lines

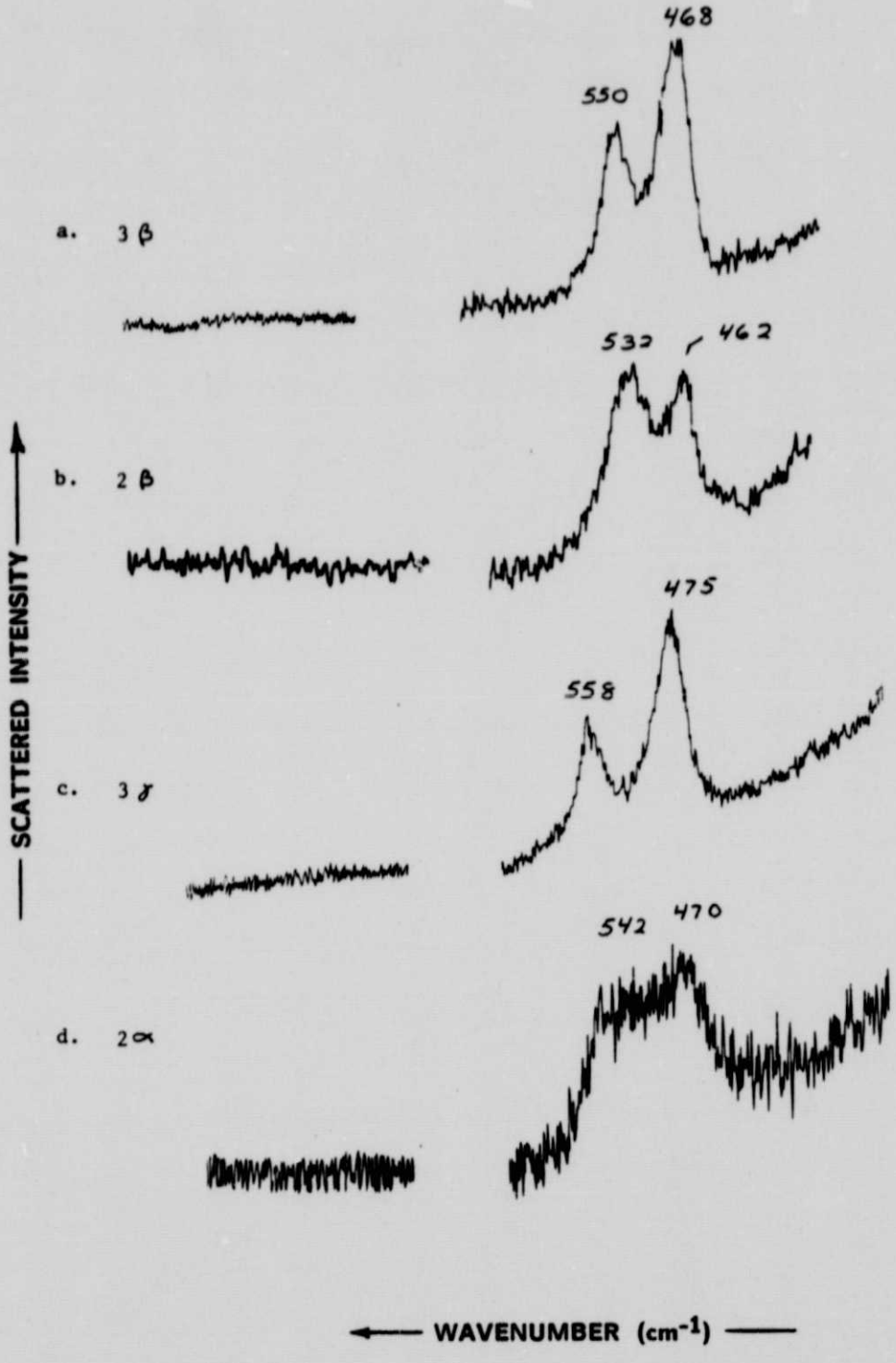

Fig. 3. Raman spectra of Electrochemical phases in OH stretching region (3500 - 3800 cm^{-1}) and lattice mode region (250 - 650 cm^{-1}).

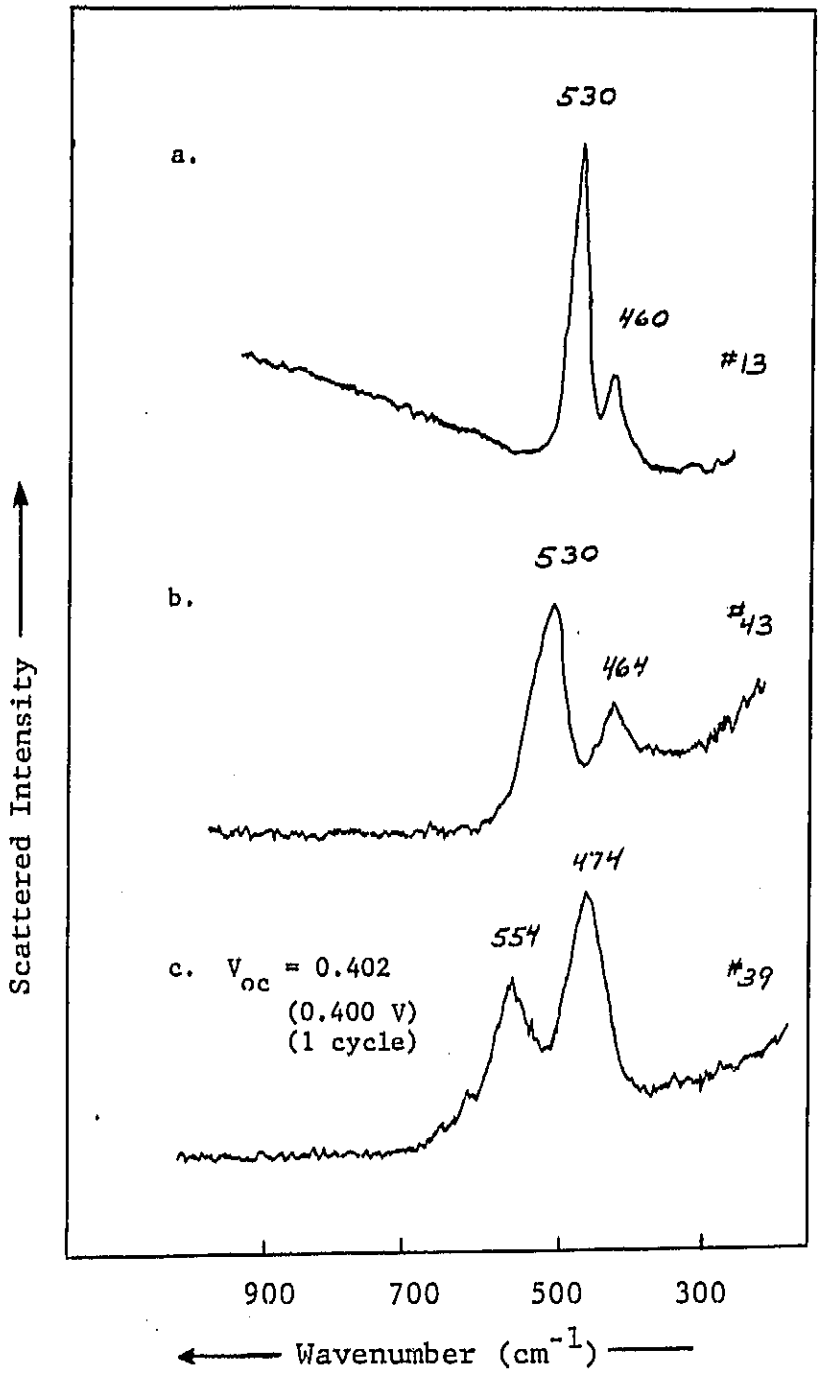

Fig. 4. Raman spectra of 10% cobalt-doped thin films: a) cathodic precipitation, b) same sample as (a) but placed in 18% KOH for one minute, and c) same type of electrode charged to V_{oc} = 0.402V.

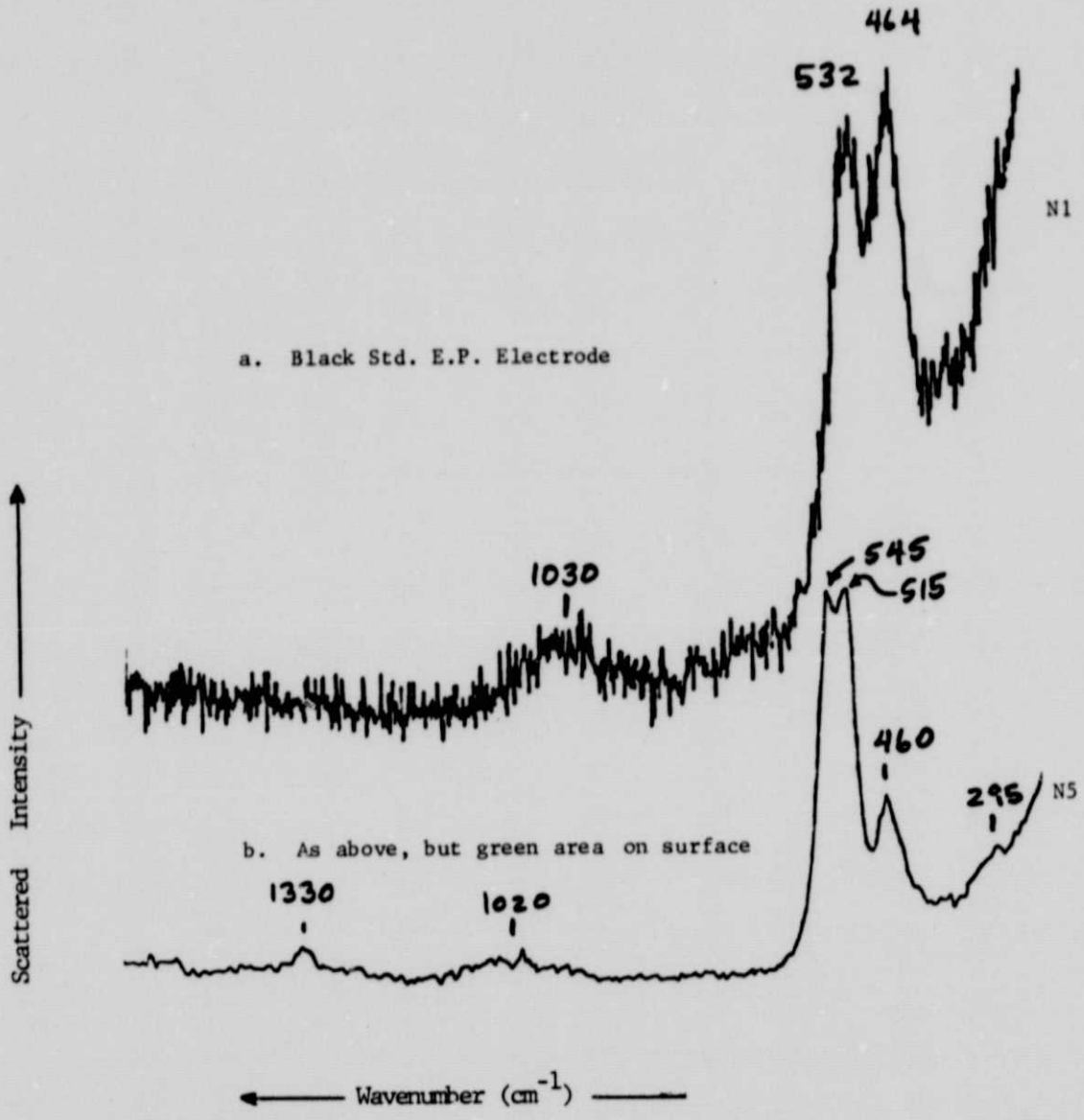

Fig. 5. Spectra from as received Eagle Picher Electrode.

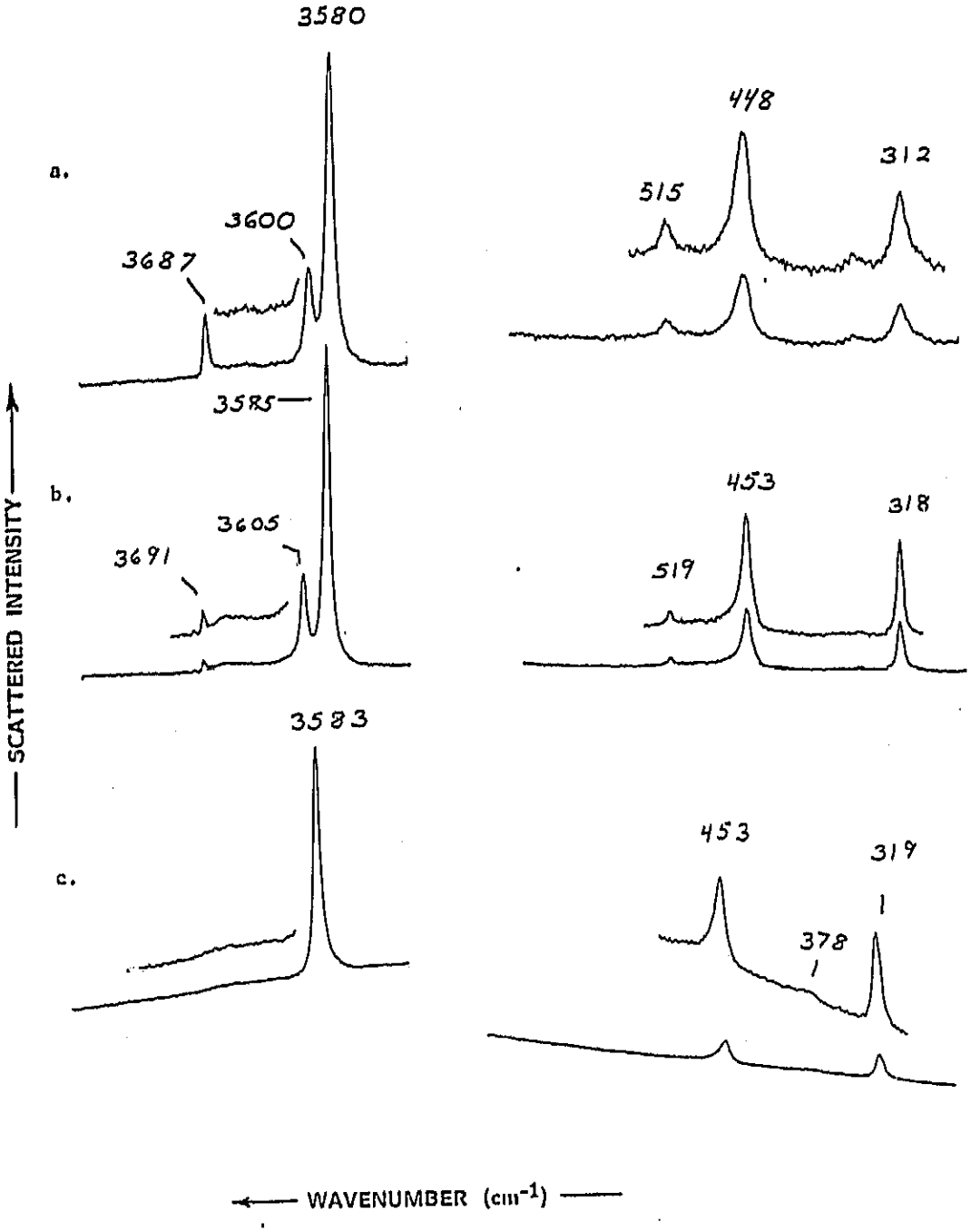

Fig. 6. Raman spectra of various preparations of β-$Ni(OH)_2$; a) initial precipitate, room temperature spectrum, b) initial precipitate, 13 K spectrum and c) recrystallized, 13 K spectrum. Same spectral regions as Fig. 3.

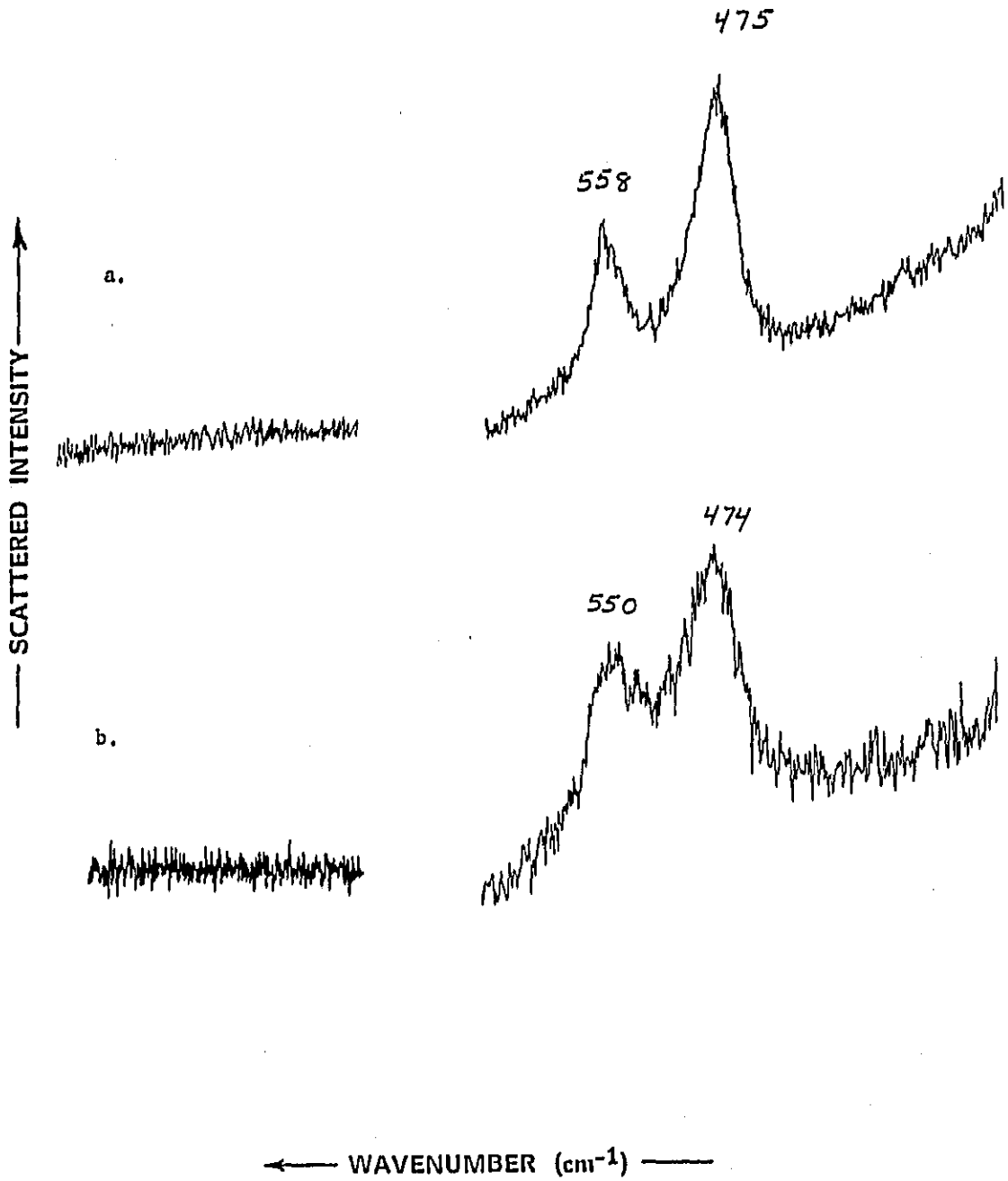

Fig. 7. Raman spectra of electrochemical 3γ - NiOOH (a) and chemically oxidized precipitate of NiOOH (b). Spectral regions as in Fig. 3.

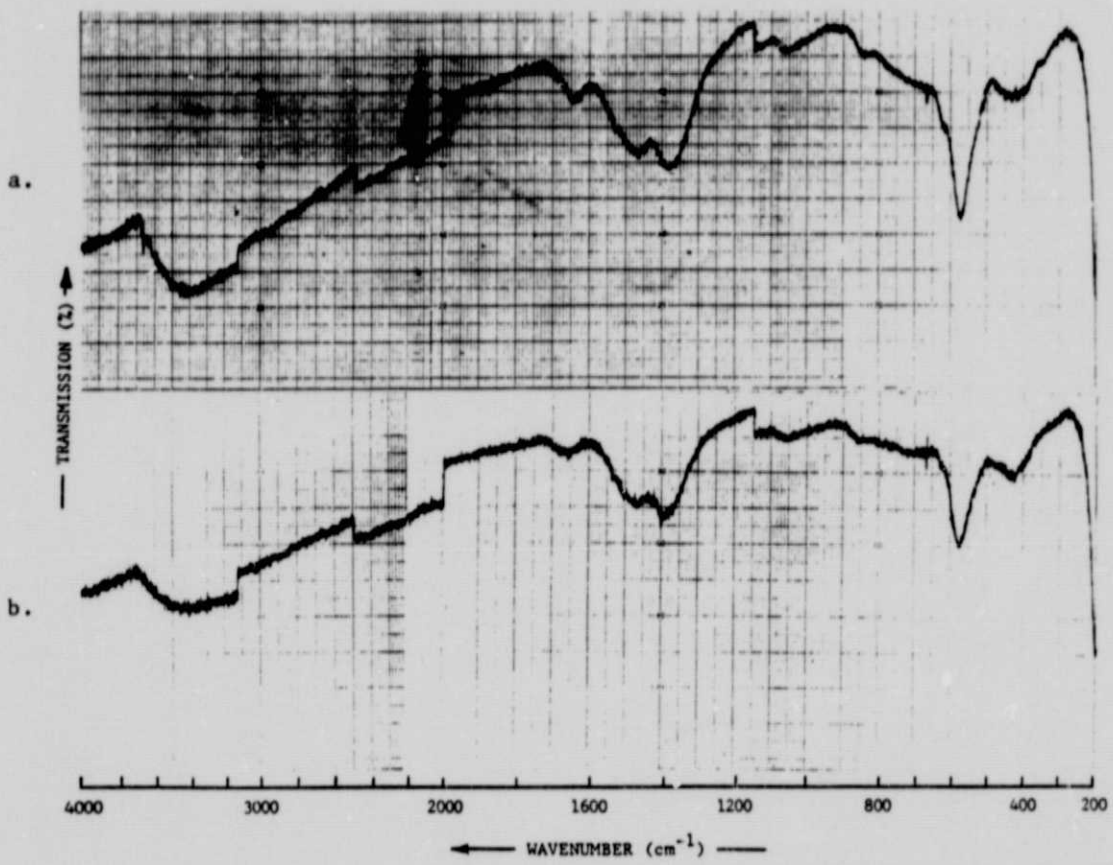

Fig. 8. Infrared spectra of electrochemical 3δ - NiOOH (a) and chemically oxidized precipitate of NiOOH (b).

TABLE I.

STRUCTURAL NOMENCLATURE

Nominal or Traditional Structure	Symbol	Origin	Color
$Ni(OH)_2$	2β	electrochemical	black
"	β	chem'l. ppt'n.	green
$Ni(OH)_2 \cdot XH_2O$	α	chem'l. ppt'n.	green
"	α	cathodic deposition	green
"	2α	electrochemical	black
"	γ	chem'l. oxid'n.	black
NiOOH	3β	electrochemical	black
"	$3\gamma, \gamma', \gamma''$	electrochemical	black
NiO	–	thermal	black or green

TABLE 2.

FACTOR GROUP ANALYSES

	β-Ni(OH)$_2$		NiOOH	
Space Group:	$P\bar{3}m - D_{3d}^3$		$R\bar{3}m - D_{3d}^5$	
Unit Cell Size:	Z=1		Z=1	
Vibrational Species:				
	Raman	IR	Raman	IR
O-H-O Modes:	A_{1g}	A_{2u}	-	A_{2u}
			-	E_u
Lattice Modes:	A_{1g}	A_{2u}	A_{1g}	A_{2u}
	$2E_g$	$2E_u$	E_g	E_u
No. Active:	4	4	2	4
No. Coincidences:	0	0	0	0

TABLE 2.

FACTOR GROUP ANALYSES

	β-$Ni(OH)_2$		NiOOH	
Space Group:	$P\bar{3}m - D_{3d}^3$		$R\bar{3}m - D_{3d}^5$	
Unit Cell Size:	Z=1		Z=1	
Vibrational Species:				
	Raman	IR	Raman	IR
O-H-O Modes:	A_{1g}	A_{2u}	-	A_{2u}
			-	E_u
Lattice Modes:	A_{1g}	A_{2u}	A_{1g}	A_{2u}
	$2E_g$	$2E_u$	E_g	E_u
No. Active:	4	4	2	4
No. Coincidences:	0	0	0	0

Table 3. Comparison of α, β, and γ literature formulae with the defective structural formulae proposed, and an example of the charging of an α-phase.[3,29,30]

Literature Formulae	Defective Structure	Average Oxidation State
α-$3Ni(OH)_2 \cdot 2H_2O$	$Ni_{0.75}(2H)_{0.25}(OOH_2)_{1.00}$	Ni^{2+}
$4NiOOH \cdot 3H_2O$	$Ni_{0.73}(3H)_{0.27}(OOH)_{1.00}$	Ni^{3+}
$4NiOOH \cdot K[O_{1.5}(OH)_{0.5}]$	$\left\{ Ni_{0.80}V_{Ni0.20}(OOH)_{0.9}(OOK_2)_{0.1} \right\}$ $\left\{ Ni_{0.80}(2K)_{0.10}(OOH)_{0.9}(OOH_2)_{0.1} \right\}$	$Ni^{3.62}$

Discharged		Charged	
M^{2+}	OOHH	M^{3+}	OOH
$[Ni_{1-x}(2H)_x]_{1.0}$	$[(OOH)H]_{1.00}$ ---->	$(Ni_{1-x}V_{Ni\,x})_{1.0}(OOH)_{1.00}$	$+ (2x+1)H^+$
$Ni_{0.75}(2H)_{0.25}$	$(OOH_2)_{1.00}$ ---->	$Ni_{0.75}V_{Ni\,0.25}(OOH)_{1.00}$	$+ 1.5\ H^+$